# Exploring the temporal variation of the solar quadrupole moment from relativistic gravitation contributions: A fortuitous circumstance?

J.P. Rozelot [a], S. Eren [b]

[a] Université Côte d'Azur, 77 Chemin des Basses Moulières, 06130 Grasse, France
[b] The Arctic University of Norway, Department of Physics and Technology, Postboks 6050 Langnes, 9037 Tromsø, Norway

Received 29 June 2019; received in revised form 29 October 2019; accepted 31 October 2019. Available online 8 November 2019

**Abstract**

Due to its oblateness, the Sun carries a solar quadrupole moment playing a key role at the crossroad of fundamental solar physics, astrometry and celestial mechanics. There is nowadays a general agreement on its order of magnitude (≈ $2\times10^{-7}$), but its temporal dependence is still poorly known. Helioseismology led to a variation within the solar cycle by less than 0.04%, not yet confirmed by other means. Analysis of the perihelion precession of planetary orbits computed in the solar equatorial coordinate system, instead of the ecliptic coordinate system usually used, shows that a periodic variation of the $J_2$ term rather than of a simple constant, must be considered. Gravity tests within the Planetary and Lunar Ephemerides provide a fruitful independent approach. Confronting results from three sets of Ephemerides computed at different periods of time, a variability dependence within the solar cycle can be evidenced. If this outcome is not fortuitous, such a finding suggests a quadratic fit, that can be explained through the variation of the rotation law with latitude and time.

Keywords: Sun: fundamental parameters; Sun: activity; Ephemerides

## 1. Introduction

For an axially symmetric distribution of rotating matter, the outer gravitational field can be expressed as:

$$\phi_{grav\ out}(r,\theta) = -\frac{GM}{r}\left[1 - \sum_{n=1}^{\infty}\left(\frac{R}{r}\right)^{2n} J_{2n}P_{2n}(\cos\theta)\right] \qquad (1)$$

where $G$ is the gravitational constant; $M$ and $R$, the mass and radius of the body; $J_{2n}$ are the gravitational multiple moments of order $n$; $P_{2n}$, the Legendre polynomials of degree $n$; $r$ and $\theta$, respectively the distance from the centre and the angle to the symmetry axis (colatitude). The first term $J_2$, for $n = 1$, is called the quadrupole moment, then for $n = 2$, $J_4$ is the hexadecapole moment, for $n = 3$, $J_6$, is the dodecapole moment, and so on. These $J_n$ coefficients are dimensionless quantities providing information on how the mass and velocity distributions act inside the body to finally render non-spherical the outer visible shape of the body. The deviation of sphericity is measured by the asphericities coefficients $c_n$, also dimensionless quantities, directly related to the coefficient of the $J_n$ in expression (1). To first order, the rotating body takes the shape of a spheroid, described by the parameter $\varepsilon$ (the flatness), and is either oblate (elongation along the equatorial axis, $n = 1$, $l = 1$ –called oblateness–), or prolate (elongation along the polar axis $n = 1$, $l = 2$ –called prolateness–; $l$ being the order; see Fig. 2 in Lefebvre et al., 2007, for a visualization of higher orders). It is straightforward to see that the oblateness $\varepsilon$ (in the general case of a fluid in rotation) is a linear function of the quadrupole and hexadecapole asphericities terms $\varepsilon = -(3/2)c_2 - (5/8)c_4$. Concerning the Sun, for which axial symmetry is generally adopted

* Corresponding author.
*E-mail address:* jp.rozelot@orange.fr (J.P. Rozelot).

https://doi.org/10.1016/j.asr.2019.10.040

(it will be the case here), $J_2$ is the most important term and should be used as a constraint in the computation of solar models, as the asphericity is a probe to test the solar interior. Further, detection of long term changes in the solar figure are intended, as there is some evidence for $J_2$ to vary with time (Emilio et al., 2007, Rozelot et al., 2009); those have been postulated to act as a potential gravitational reservoir that can be a source of solar luminosity variation. The mechanism described in Pap et al., 1998, 2001, and Jain et al. (2018) is as follows. The ultimate source of solar energy is provided by nuclear reactions taking place in the center of the Sun; the rate of these reactions is almost constant on the time scales of millions of years. On the other hand, solar phenomena observed at the surface show variations on time scale from minutes to centuries. If the central energy source remains constant while the rate of energy emission from the surface varies, thus, there must be an intermediate reservoir (or intermediate factors) where the energy can be stored or released. The gravitational field of the Sun is one such energy reservoir. If the energy is stored there, it will result a change in the solar radius (Pap et al., 2001; Fazel et al., 2008). Thus, a careful determination of the time dependence of the solar radius over all latitudes (i.e. the determination of the solar shape) can provide a constraint not only on models of total irradiance variations (Pap et al., 2001; Jain et al., 2018), but also on models involving the near sub-surface layer (NSSL or "leptocline"; see for instance Godier and Rozelot, 2001, Reiter et al., 2015 –end of § 7), or even down to the solar core.

Solar gravitational moments of higher degree than 2, are nearly null. However, still assuming the axial symmetry, $J_2$ and $J_4$ are related to $\varepsilon$ through the relation (to first order) $J_4 = \left(-\frac{4}{5}\varepsilon^2 + \frac{4}{7}\varepsilon m\right)$ where $m$ is the ratio of the centrifugal force to gravity at the equator.

The first time that the solar quadrupole moment was associated with the gravitational motion of Mercury was in 1895. Newcomb (1895) attempted to account for the anomalous perihelion advance of this planet with a modified gravitational field manifested by an oblateness $\varepsilon$ of the Sun (the difference between the equatorial and polar radius $\Delta r$, reported to the equatorial one). Indeed, in 1859, Le Verrier had observed a deviation of Mercury's orbit from Newtonian predictions, which could not be due to the presence of known planets. But, solar observations soon ruled out the difference between the equatorial and polar diameters of the Sun of $\Delta r = 500$ mas (milli-arc-sec), as advocated by Newcomb. And Einstein's new theory of gravitation, General Relativity, could account for almost all the observed perihelion advance. So, Mercury's perihelion advance readily became one of the cornerstones for testing General Relativity. However, a contribution to the perihelion shift from the solar figure (though very less important than first suggested by Newcomb) can not be discarded.

This paper is organized as follows. We first briefly describe the solar quadrupole moment $J_2$ in light of the explanation above. Then focus on the available Ephemerides data and how a temporal dependence of $J_2$ from Mercury data can be extracted. Following that we discuss the results attempt to explain the temporal variation of solar quadrupole moment.

## 2. The solar quadrupole moment

It has been recognized that the observed solar oblateness is stronger than the oblateness estimated from the mean solar rotation. This excess is due to the existence of a gravitational quadrupole moment $J_2$. Today there is a general agreement that its order of magnitudes set at $\approx (2.0 \pm 0.4) \times 10^{-7}$. However, the question of temporal dependence is absolutely not umpired as (i) observations are at the cutting edge of the techniques and (ii) the mapping of the surface magnetic fields, which could produce a supplementary shape distortion (or not) due to the rotation, is not known with sufficient accuracy to be properly modeled. The same approach goes for potential other factors such as turbulent pressure, shear effects, or other stresses, which could contribute to affect the solar shape. However, contemporary measurements of the solar shape made by means of the MDI-SoHO experiment (Scherrer et al., 1995) or by the Helioseismic and Magnetic Imager (HMI) instrument onboard the Solar Dynamics Observatory (SDO) (Scherrer et al., 2012), indicate a temporal variability of the asphericities coefficients (Emilio et al., 2007; Kuhn et al., 2012, Kosovichev and Rozelot (2018a,b)). Even if the contribution of the solar limb shape is a few percent of those due to the gravitational moments, a temporal variability is expected. Surely, determining their order of magnitude this way requires high sensibility methods.

Helioseismology provided the premises for a variation of the gravitational moments associated with the solar cycle. The amplitude modulation is less than 0.04% (Antia et al., 2008) for $J_2$ and such a tiny modulation has not been confirmed so far. Therefore, the contribution of the gravitational moment to the advance of the Mercury perihelion as described above provides an independent and productive method. Limiting ourselves here to $n = 2$, the analysis of results deduced from Planetary Ephemerides enables us to determine an estimate of the solar quadrupole moment leading to an unexpected result.

## 3. Progress made through the advent of new Ephemerides

Various authors have independently developed high precision of Lunar and Planetary Ephemerides, which has served as a basis to set up celestial and nautical almanacs. They are considered as a worldwide resource for fundamental astronomical data, often being the first publications to incorporate new International Astronomical Union resolutions. Planetary Ephemerides are developed on the basis of numerical integration of the motion of the nine planets and the Moon fitted to the most accurate available observations. They progressively integrated the motion of perturbing main belt asteroids (up to 300), the Earth's rotation and Moon libration. The accuracy obtained by successive versions are compared with previous one and with the solutions obtained (e.g. Park et al., 2017; Genova et al., 2018). We used here ephemerides for which there is a complete consistency of the dynamical modeling since Earth rotation, Moon libration and asteroid orbits are integrated with the main equations of the planetary motions (see for instance a discussion by Hilton and Hohenkerk, 2010).

Three major centers continue to maintain high accurate Ephemerides:

- The Ephemerides of Planets and the Moon (EPM), first created in the 1970s to support Russian space flight missions, is constantly improved at the Institute of Applied Astronomy (IAA–RAS) in Saint-Petersburg (Russia);
- The Jet Propulsion Laboratory (JPL, Pasadena, Ca, USA) is considered as a fundamental laboratory for building and operating accurate Ephemerides (called DE), which paved the way for planetary missions and allows for defining highly accurate spacecrafts trajectories;
- The "Institut de Mécanique Céleste et de Calcul des Ephémérides" (IMCCE-Paris, F) has been developing analytical solutions for the motions of planets, called "Intégration Numérique Planétaire de l'Observatoire de Paris" (INPOP), since the early 1980s.

High precision observations through different means (Lunar Laser Ranging, radar observations of the inner planets, radio tracking measurements of spacecrafts in orbit around planets, Very Long Base Interferometry...) allows for the determination of orbits of the planets with an uncertainty of a few hundred meters. Such accuracy can be achieved by taking into account the relativistic gravitational contribution. The main and best determined relativistic effect in the solar system is the secular advance of the perihelion of Mercury ($\Delta\omega$), which is known to depend on a linear combination of the Post–Newtonian Parameters $\beta$ and $\gamma$ and on the gravitational quadrupole moment of the Sun $J_2$ over the form $\Delta\omega = f(\beta, \gamma) + g(J_2)$. The first term is proportional to the semi major axis of the planet, while the second is proportional to its square. Thus, $J_2$ can, in principle, be determined using data from different planets. However, these three parameters are highly correlated, and even with additional constraints, such as the periodic effect on the perihelion motion, disentangling the complex data still remains a difficult task. As far as $J_2$ (sometimes called oblateness, but it is an abuse of language as seen before) is concerned, its temporal variation requires further consideration, as it is still taken as a constant in planetary orbits studies.

Since advances in techniques for deep space exploration in the solar system have improved and since tracking spacecrafts have provided the higher precision data sets with more sophisticated data analysis, it would be more logical to expect that the estimates of the solar gravitational moments (and their respective accuracies) would be also improved.

Based on available results (from 1996 to 2017, inferred from the same selected techniques), it seems that it is not the case. As a first step, we may display the $J_2$ estimates at the date they were obtained. If $J_2$ is constant, we should get a trend, inside the error bars, which should reflect the better accuracy obtained over time through the measuring instruments and through that of the data analysis. To take into account a better tagging, we selected the date at which the data were analyzed for the first time with the help of a more accurate ephemerides. In principle, such new computations should lead to an increasingly accurate value of $J_2$. Or maybe, they will present an erratic distribution (within the whole range of known values) which could reflect the different techniques used or the means of analysis. We are aware that solutions obtained by the different authors do not have exactly the same modeling, nor exactly the same set of fitted observations. Values and uncertainties provided by the different solutions must be combined with caution. However, the process can be assumed to be nearly

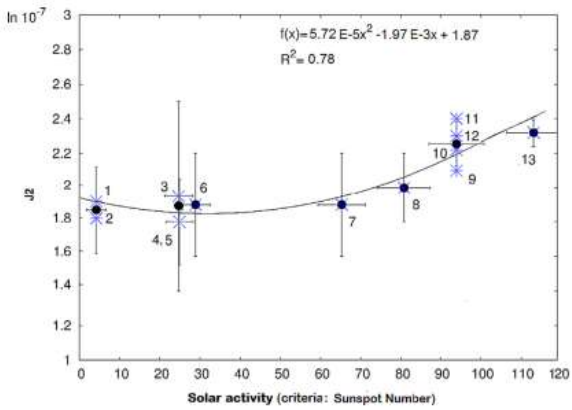


Fig. 1. Solar quadrupole moment $J_2$ versus the solar activity. The best fit is a quadratic curve, meaning a temporal signature, that can be explained by the dependence of the gravitational moment with the square of the rotation. Points marked as a cross are as followed ($J_2$ in $10^{-7}$): 1. EPM2008: ($1.92 \pm 0.30$) (Pitjeva, 2014a); 2. INPOP08: ($1.82 \pm 0.47$) (Fienga et al., 2011); 3. INPOP06: ($1.95 \pm 0.55$) (Fienga et al., 2011); 4. DE423 (created February 2010); (1.80) (Verma et al., 2014); 5. INPOP10e: ($1.8 \pm 0.25$) (Verma et al., 2014); 6. DE405 (created May 1997): ($1.9 \pm 0.3$) (Standish, 1998); 7. EPM2004: ($1.9 \pm 0.3$) (Pitjeva, 2005; Pitjeva, 2013); 8. EPM2011: ($2.0 \pm 0.2$) (Pitjeva, 2014a); 9. DE430 (created April 2013): ($2.1 \pm 0.7$) (Williams et al., 2013); 10. EPM2013: ($2.22 \pm 0.23$) (Pitjeva and Pitjev, 2014b); 11. INPOP13a: ($2.40 \pm 0.20$) (Verma et al., 2014); 12. INPOP13c: ($2.3 \pm 0.25$) (Fienga et al., 2015). 13. JPL Ephemerides using MESSENGER data ($2.26 \pm 0.09$) (Park et al., 2017). Points marked as a circle are the values weighted by their errors, obtained when several estimated values are produced at the same epoch. The obtained quadratic fit is in accordance with a temporal variation of $J_2(t)$ which can be set up as a function of $(\Omega^2(t))$ where $\Omega$ is the (complex) time dependent solar rotation rate.

V

Table 1
List of the Ephemerides used in this study sorted by their date of creation and the deduced estimates of the solar quadrupole moment $J_2$ with their uncertainties. IAA: Institute of Applied Astronomy in Saint Petersburg (Russia). IMCCE: Institut de Mécanique Céleste et de Calcul des Ephémérides in Paris (F). INPOP13c is an upgraded version of INPOP13a, fitted to LLR (Laser Lunar Ranging) observations, including new observations of Mars and Venus deduced from MEX, Mars Odyssey and VEX tracking data.

| Name of the ephemeris & Institute | Creation date of the ephemeris | Quadrupole moment (in $10^{-7}$) | Author & Reference |
|---|---|---|---|
| DE405 JPL (USA) | May 1997 | $1.9 \pm 0.3$ | Standish (1998) |
| EPM2004 IAA (Russia) | 2004 | $1.9 \pm 0.3$ | Pitjeva (2005); Pitjeva (2013) |
| INPOP06 IMCCE (F) | 2006 | $1.95 \pm 0.55$ | Fienga et al. (2011) |
| EPM2008 IAA (Russia) | 2008 | $1.92 \pm 0.30$ | Pitjeva (2014a) |
| INPOP08 IMCCE (F) | 2008 | $1.82 \pm 0.47$ | Fienga et al. (2011) |
| DE423 JPL (USA) | February 2010 | 1.80 | Verma et al. (2014) |
| INPOP10e IMCCE (F) | 2010 | $1.8 \pm 0.25$ | Verma et al. (2014) |
| EPM2011 IAA (Russia) | 2011 | $2.0 \pm 0.2$ | Pitjeva (2014a) |
| DE430 JPL (USA) | April 2013 | $2.1 \pm 0.7$ | Williams et al. (2013) |
| EPM2013 IAA (Russia) | 2013 | $2.22 \pm 0.23$ | Pitjeva and Pitjev, (2014b) |
| INPOP13a IMCCE (F) | 2013 | $2.40 \pm 0.20$ | Verma et al. (2014) |
| INPOP13c IMCCE (F) | 2013 | $2.3 \pm 0.25$ | Fienga et al. (2015) |
| *MESSENGER JPL (USA)* | 2012–2014 | $2.26 \pm 0.09$ | Park et al. (2017). |

the same, and if $J_2$ is constant, then we expect to get a mean value within the (decreasing) error bars.

Results are shown in Fig. 1. Surprisingly, the data adjust a temporal law. Is this fortuitous? Bearing in mind that the solar moments could be related to solar activity, and $J_2$ at first, we wondered what role a temporal dependence of this parameter could play in the determination of the ephemerides. In other words, the analysis may encapsulate the temporal variations of $J_2$ and so, the determined value is the result of what was significantly in progress within the activity of the Sun. Then $J_2$ will be more affected by the solar properties than by the relativistic effects (and does the non-decorrelated $J_2$ with $[\beta, \gamma]$ not introduce a bias?). Although each ephemerides is the output of a different complex least-square analysis over a long period of solar system orbital motions, nevertheless, we can conjecture that $J_2$ acts as a constraint due to the solar activity. Fig. 1, where the estimate of the solar quadrupole moment has been plotted as a function of the solar activity, characterized by the yearly mean sunspot number (Clette et al., 2015) defined at the time of each run made over the considered ranging period (labeled 1 to 13, see the caption), shows this remarkable and unexpected correlation.

Except for MESSENGER[1] data, we are noting that the determination of $J_2$ does not take into account the Lense–Thirring Precession (Iorio, 2012). Indeed the non–modeled gravitomagnetic effects are totally removed from the post–fit signature in the data–reduction process of the Planetary and Lunar Ephemerides in the above mentioned processes. However the Lense–Thirring effect can be estimated at $\approx$(-) 6–7%, so that the precedent correlation is solely affected by a (down) translation. It results that the quadratic curve obtained would better adjust point 13 (we took here subset 1 as indicated in Table 1 (Park et al., 2017), up to August 2014 to take advantage of a bigger solar activity; other data does not change significantly the result). However, this data set induced a bias due to its separation into two subsets of time (the first one from 2011 March through 2012 September, and the second one from 2012 September to 2014 August). Therefore, it has been considered for the statistics computed for determining the significant level of correlation arising between $J_2$ and the sunspot number only as an indicative point (Table 1).

Genova (2018), using data from the NASA MESSENGER mission, collected over the years 2008–2015 (around 2/3 of the solar cycle), retrieved a mean solar gravitational moment $J_2 = (2.246 \pm 0.022) \times 10^{-7}$. The analysis is slightly different than the previous methods used and thus, we do not incorporate this result in our study (to validate the results, the orbit of Mercury was reintegrated to adjust again the values; the whole process is thus not fully comparable with other data used in this study).

### 3.1. Discussion

Is the found quadratic fit significantly better than a constant or a linear trend? To explore this issue, we did sixteen successive tests, according to the way the $J_2$ fit was obtained. The first combination considered $J_2$ as a function of the date, i.e. the time at which runs of the ephemerides were made for the first time. A linear trend and a quadratic curve are deduced each time to fit the data. The second combination was made by considering $J_2$ as a function of the sunspot number, and a linear and quadratic fit can be performed as well. Since $J_2$ was sometimes produced on a same date, we computed the mean, weighted by the errors, for these specific epochs. The fifth and sixth combinations were built the same way as above.

For each combination, noted respectively as (a), (b), (c), (d), (e), (f), (g), (h) and (i), we computed the successive

[1] MErcury Surface, Space ENvironment, GEochemistry, and Ranging spacecraft in orbit about Mercury operating to estimate the precession of Mercury's perihelion.

Pearson coefficients and their associated Student $t$ test to check the null hypothesis. We took, as usual, a significant level $P$ at 0.05. To be complete, but given here as an indicative issue, we added one data set from Messenger, according to the same principles as above mentioned. The resulting models are called (i), (j), (k), (l) and for the weighted estimates (m), (n), (o) and (p).

The Student-$t$ table gives 2.228, 2.571, 2.201 and 2.447 as the critical threshold for 10, 5, 11 and 6 freedom degrees corresponding respectively to models (a,b,c,d), (e,f, g, h), (i, j, k, l) and (m, n, o, p). Results are given in Table 2.

Table 2 shows that quadratic fits are in any case better than linear trends. The best correlation is obtained with a quadratic fit linking $J_2$ with solar activity (model d). The relative direct amplitude of the variation found appears to be approximately 0.18, a value which may seem a little bit high. However, this estimate must be nuanced: in a period of low solar activity, up to a sunspot number of $\approx 70$, the variation is around 0.10 and rises to around 0.15 in a period of higher activity. Interestingly, $J_2$ is anti-correlated with solar activity when this one is low, and correlated for higher periods of activity. All linear trends with dates are moderately acceptable, at least at a significant level of 95% probability.

Fig. 1 shows also that a value of $J_2$ taken as a constant of around 2.1 (2.08 exactly) crosses the observed values except for some points, for which the line is quite exactly at the superior or inferior borders of the error bars. We thus performed a distribution $t$ test to check if this constant value could be significant. For an expected value $m$, the variance $S_x$ is estimated as $(\sigma/\sqrt{N}) \times \sqrt{1-1/\mu}$, where $N$ is the length of the sample, $\sigma$ the standard deviation and $\mu$ the subset of independent values. Admitting the normality of the random variable $t = [\bar{x} - m]/S_x$, one obtains $t =$ 0.054(9) for 12 points and 0.054(2) for 13 points (note that $\overline{J_2}$ is respectively 2.01 and 2.03). It results that the confidence intervals are respectively [1.96–2.06] and [1.97–2.08] at the level of 95% probability. Thus, the constant value of 2.08 cannot be viewed as good enough in the first case and appears as marginal in the second one.

Lastly, a model of degree 2 could better fit the observed points than a linear trend; by increasing the degree $n$ of the fitting polynomial, the model could pass to all the points. The question which may arise is to which degree the process has to be stopped, the fitting becoming no more relevant. All the observed values being considered, the correlation coefficients obtained are as followed, from $n = 1$ to $n = 6$:

$r_n = 0.85 \quad 0.88 \quad 0.89 \quad 0.92 \quad 0.93 \quad 0.93$

We compare the successive $r_{n+1}, r_{n+2}, r_{n+3}$ (...) to $r_{n=1}$, i.e. forming the differences $\delta r_i$ and then applying the Fisher transformation $\delta r'_i$. The statistic test is classically chosen as $Z = (1/E)\delta r'_i$ with $E^2 = 2 \times (1/df)$ where $df = 10$ is the degree of freedoms. We obtain $Z = 0.293$, 0.389, 0.782, 0.918 and 0.918, showing that we can stop at $n = 3$ at a 95% probability (as Student bilateral table gives 0.775, 0.705, 0.452, 0.380 and 0.380). Models of degree 4 and higher gives a better correlation coefficient, but the statistics are not significantly increased. However, a model of degree 3 (and higher) would be difficult to interpret.

*This new temporal variation of $J_2$ begs explanation.* A further paper will explore in more details, and on an other basis, why and how $J_2$ should not be expressed as a constant. We just want to note here that $J_2$ varies, at least in the first order, as the square of the solar latitudinal surface rotation rate $\Omega$, which is a function of time. The visual oblateness $\Delta_s$ is described by $\Delta_s = -\frac{3}{2}J_2 + \frac{\Omega^2 R_\odot^3}{2GM_\odot}$, where $R_\odot, M_\odot$ and $G$ have their usual meaning. $\Omega$ is an ill–defined characteristic as it is a quadratic function of the colatitude $\theta$, under the form $\Omega = A + Bcos^2(\theta) + Ccos^4(\theta)$. As the

Table 2
Statistics computed for different combinations linking the solar quadrupole moment temporal variations as a function of either the date or the solar activity. A linear trend and quadratic fit is obtained for each model. SN stands for Sunspot Number and "pond." for "mean weights by their errors".

| Model | Pearson coefficient | Student $t$ test | Result |
|---|---|---|---|
| (a- $J_2$ date linear) | 0.54(9) | 2.076 | Rejected |
| (b- $J_2$ date quadratic) | 0.79(0) | 4.076 | Acceptable |
| (c- $J_2$ SN linear) | 0.82(6) | 4.633 | Acceptable |
| (d- $J_2$ SN quadratic) | 0.88(3) | 6.245 | Fairly good |
| (e-pond. $J_2$ date linear) | 0.47(3) | 1.201 | Rejected |
| (f-pond. $J_2$ date quadratic) | 0.72(7) | 2.366 | Rejected |
| (g-pond. $J_2$ SN linear) | 0.74(4) | 2.408 | Rejected |
| (h-pond. $J_2$ SN quadratic) | 0.90(0) | 4.627 | Acceptable |
| Including one data set from | Messenger | (ref: Park et al. (2017)): | |
| (i- $J_2$ date linear) | 0.59(7) | 2.465 | On the border |
| (j- $J_2$ date quadratic) | 0.82(1) | 4.761 | Acceptable |
| (k- $J_2$ SN linear) | 0.85(1) | 5.369 | Good |
| (l- $J_2$ SN quadratic) | 0.88(8) | 6.394 | Fairly good |
| (m-pond. $J_2$ date linear) | 0.60(7) | 1.870 | Rejected |
| (n-pond. $J_2$ date quadratic) | 0.83(4) | 3.707 | Acceptable |
| (o-pond. $J_2$ SN linear) | 0.83(7) | 3.749 | Acceptable |
| (p-pond. $J_2$ SN quadratic) | 0.90(7) | 5.278 | Good |

Pearson coefficients and their associated Student $t$ test to check the null hypothesis. We took, as usual, a significant level $P$ at 0.05. To be complete, but given here as an indicative issue, we added one data set from Messenger, according to the same principles as above mentioned. The resulting models are called (i), (j), (k), (l) and for the weighted estimates (m), (n), (o) and (p).

The Student-$t$ table gives 2.228, 2.571, 2.201 and 2.447 as the critical threshold for 10, 5, 11 and 6 freedom degrees corresponding respectively to models (a,b,c,d), (e,f, g, h), (i, j, k, l) and (m, n, o, p). Results are given in Table 2.

Table 2 shows that quadratic fits are in any case better than linear trends. The best correlation is obtained with a quadratic fit linking $J_2$ with solar activity (model d). The relative direct amplitude of the variation found appears to be approximately 0.18, a value which may seem a little bit high. However, this estimate must be nuanced: in a period of low solar activity, up to a sunspot number of $\approx$70, the variation is around 0.10 and rises to around 0.15 in a period of higher activity. Interestingly, $J_2$ is anti-correlated with solar activity when this one is low, and correlated for higher periods of activity. All linear trends with dates are moderately acceptable, at least at a significant level of 95% probability.

Fig. 1 shows also that a value of $J_2$ taken as a constant of around 2.1 (2.08 exactly) crosses the observed values except for some points, for which the line is quite exactly at the superior or inferior borders of the error bars. We thus performed a distribution $t$ test to check if this constant value could be significant. For an expected value $m$, the variance $S_x$ is estimated as $(\sigma/\sqrt{N}) \times \sqrt{1 - 1/\mu}$, where $N$ is the length of the sample, $\sigma$ the standard deviation and $\mu$ the subset of independent values. Admitting the normality of the random variable $t = [\bar{x} - m]/S_x$, one obtains $t =$ 0.054(9) for 12 points and 0.054(2) for 13 points (note that $\overline{J_2}$ is respectively 2.01 and 2.03). It results that the confidence intervals are respectively [1.96–2.06] and [1.97–2.08] at the level of 95% probability. Thus, the constant value of 2.08 cannot be viewed as good enough in the first case and appears as marginal in the second one.

Lastly, a model of degree 2 could better fit the observed points than a linear trend; by increasing the degree $n$ of the fitting polynomial, the model could pass to all the points. The question which may arise is to which degree the process has to be stopped, the fitting becoming no more relevant. All the observed values being considered, the correlation coefficients obtained are as followed, from $n = 1$ to $n = 6$:

$r_n = 0.85 \quad 0.88 \quad 0.89 \quad 0.92 \quad 0.93 \quad 0.93$

We compare the successive $r_{n+1}, r_{n+2}, r_{n+3}$ (...) to $r_{n=1}$, i.e. forming the differences $\delta r_i$ and then applying the Fisher transformation $\delta r_i'$. The statistic test is classically chosen as $Z = (1/E)\delta r_i'$ with $E^2 = 2 \times (1/df)$ where $df = 10$ is the degree of freedoms. We obtain $Z = 0.293$, 0.389, 0.782, 0.918 and 0.918, showing that we can stop at $n = 3$ at a 95% probability (as Student bilateral table gives 0.775, 0.705, 0.452, 0.380 and 0.380). Models of degree 4 and higher gives a better correlation coefficient, but the statistics are not significantly increased. However, a model of degree 3 (and higher) would be difficult to interpret.

*This new temporal variation of $J_2$ begs explanation.* A further paper will explore in more details, and on an other basis, why and how $J_2$ should not be expressed as a constant. We just want to note here that $J_2$ varies, at least in the first order, as the square of the solar latitudinal surface rotation rate $\Omega$, which is a function of time. The visual oblateness $\Delta_s$ is described by $\Delta_s = -\frac{3}{2}J_2 + \frac{\Omega^2 R_\odot^3}{2GM_\odot}$, where $R_\odot, M_\odot$ and $G$ have their usual meaning. $\Omega$ is an ill–defined characteristic as it is a quadratic function of the colatitude $\theta$, under the form $\Omega = A + Bcos^2(\theta) + Ccos^4(\theta)$. As the

Table 2
Statistics computed for different combinations linking the solar quadrupole moment temporal variations as a function of either the date or the solar activity. A linear trend and quadratic fit is obtained for each model. SN stands for Sunspot Number and "pond." for "mean weights by their errors".

| Model | Pearson coefficient | Student $t$ test | Result |
|---|---|---|---|
| (a- $J_2$ date linear) | 0.54(9) | 2.076 | Rejected |
| (b- $J_2$ date quadratic) | 0.79(0) | 4.076 | Acceptable |
| (c- $J_2$ SN linear) | 0.82(6) | 4.633 | Acceptable |
| (d- $J_2$ SN quadratic) | 0.88(3) | 6.245 | Fairly good |
| (e-pond. $J_2$ date linear) | 0.47(3) | 1.201 | Rejected |
| (f-pond. $J_2$ date quadratic) | 0.72(7) | 2.366 | Rejected |
| (g-pond. $J_2$ SN linear) | 0.74(4) | 2.408 | Rejected |
| (h-pond. $J_2$ SN quadratic) | 0.90(0) | 4.627 | Acceptable |
| Including one data set from | Messenger | (ref: Park et al. (2017)): | |
| (i- $J_2$ date linear) | 0.59(7) | 2.465 | On the border |
| (j- $J_2$ date quadratic) | 0.82(1) | 4.761 | Acceptable |
| (k- $J_2$ SN linear) | 0.85(1) | 5.369 | Good |
| (l- $J_2$ SN quadratic) | 0.88(8) | 6.394 | Fairly good |
| (m-pond. $J_2$ date linear) | 0.60(7) | 1.870 | Rejected |
| (n-pond. $J_2$ date quadratic) | 0.83(4) | 3.707 | Acceptable |
| (o-pond. $J_2$ SN linear) | 0.83(7) | 3.749 | Acceptable |
| (p-pond. $J_2$ SN quadratic) | 0.90(7) | 5.278 | Good |

coefficients $A, B$ and $C$ are time dependent (Lustig, 1983; Balthasar et al., 1986; Javaraiah, 2003; Susuki, 2012), so is $\Omega$, and hence $J_2$. Armstrong and Kuhn (1999) have provided a more sophisticated analysis, taking into account the non uniform rotation over latitudinal cylinders. However, these authors have claimed that "the quadrupole (and hexadecapole) limb shape are mildly inconsistent with current solar rotation models" and that the discrepancy will probably be removed by a better understanding of the solar core rotation. Progress on this problem will depend on improved measurements of the limb shape, but also by a better understanding of the two-dimensional solar interior rotation rate. Lastly, these effects are likely to be detectable by the BepiColombo mission around Mercury, for which launch has been made in 2018 (see for instance Schettino et al., 1983) and results are expected in the near future.

## 4. Conclusion

The gravitational moments of the Sun influence the motion and inclination of the planetary orbits. The first one ($J_2$) significantly changes the dynamics of the inner planets, especially Mercury, for which many studies have been conducted. Increasing accuracy in the techniques helps us to take into account the outer planets Jupiter, Saturn. We could even consider new distant planet (the so-called Telisto/PlanetNine (Brown and Batygin, 2016)) since it would induce a subtle additional perihelion precession for biasing the recovery of the quadrupole moment, or mimic it (Iorio, 2017).

We have shown here that even if the orders of magnitude are very faint, implying a difficulty to disentangle the different parameters involved in the secular trends which are induced precisely by this solar gravitational mass, it is possible to derive a quadratic variation of $J_2$ with time. Higher orders of the multipole may have a non negligible impact on the perihelion precessions as some of them could have a larger temporal dependence (Antia et al., 2008).

Xu et al. (2017) studied the secular solutions for the oblateness disturbance, in consideration of the periodic variation of the $J_2$ term to derive the perihelion precession of Mercury. The results show that the temporal dependence of $J_2$ has an effect of nearly 0.8 per cent of the secular perihelion precession of Mercury.

The process described here (from non local theories of the gravitation allowing for deduction of the solar gravitational moment by fitting the observed Ephemerides to computations) is fully independent from other methods, such as the helioseismology one. Let us recall that the mean (weighted) $J_2$ value obtained by the analysis of the f–modes leads to $(2.16 \pm 0.06) \times 10^{-7}$ (in grouping the values obtained by Paternò et al. (1996), Pijpers, 1998 and Godier and Rozelot, 2001), i.e. respectively (in $10^{-7}$), 2.08 $\pm$ 0.14, 2.18 $\pm$ 0.06 and 2.0 $\pm$ 1.4), compatible with the mean weighted value obtained here $(2.17 \pm 0.06) \times 10^{-7}$ and those of Pireaux and Rozelot (2003), i.e. $J_2 = (2.00 \pm 0.40) \times 10^{-7}$. All these values are independent from the ones quoted in this paper (in Fig. 1, and in Genova et al., 2018 –noticing $J_2$ is not the solar oblateness).

The $J_2$ solar cycle variation found here, adds a new insight into solar gravitational moments, an adventure which began more than 45 years ago, when Dicke (1970) first proposed that the Sun may have a distorted interior induced by a rapidly rotating core, a fossil remnant of the rotation of the young Sun. Such a rapid core rotation was rediscovered by Fossat et al. (2017) by means of helioseismic data.

## Declaration of Competing Interest

The authors declare that they have no known competing financial interests or personal relationships that could have appeared to influence the work reported in this paper.

## Acknowledgments

The authors thank the referees for their very helpful comments. One of us (JPR) acknowledges the Arctic University of Norway, Department of Physics and Technology, for allocating time in this research.

## References

Antia, H.M., Chitre, S.M., Gough, D.O., 2008. Temporal variations in the Sun's rotational kinetic energy. Astron. Astrophys. 477, 657–663. https://doi.org/10.1051/0004-6361:20078209.

Armstrong, J., Kuhn, J.R., 1999. Interpreting the solar limb shape distortions. Astrophys. J. 525, 533–538. https://doi.org/10.1086/30787.

Balthasar, H., Vazquez, M., Wöhl, 1986. Differential rotation of sunspot groups in the period from 1874 through 1976 and changes of the rotation velocity within the solar cycle. Astron. Astrophys. 155, 87–98.

Clette, F., Cliver, E.W., Lefèvre, L., Svalgaard, L., Vaquero, J.M., 2015. Revision of the Sunspot Number(s). Space Weather 13, 529–530. https://doi.org/10.1002/2015SW001264.

Brown, M.E., Batygin, K., 2016. Observational constraints on the orbit and location of planet nine in the outer solar system astrophys. J. Lett. 824 (2), L23. https://doi.org/10.3847/2041-8205/824/2/L23.

Dicke, R.H., 1970. Internal rotation of the sun. Ann. Rev. Astron. 8, 297–328. https://doi.org/10.1146/annurev.aa.08.090170.001501.

Emilio, M., Bush, R.I., Kuhn, J., Scherrer, P., 2007. A changing solar shape. Astrophys. J. Lett. 660, L161–L163. https://doi.org/10.1086/518212.

Fazel, Z., Rozelot, J.P., Lefebvre, S., Ajabshirizadeh, A., Pireaux, S., 2008. Solar gravitational energy and luminosity variations. New Astron. 13, 65–72. https://doi.org/10.1016/j.newast.2007.05.003.

Fienga, A., Laskar, J., Kuchynka, P., Manche, H., Desvignes, G., Gastineau, M., Cognard, I., Theureau, G., 2011. The INPOP10a planetary ephemeris and its applications in fundamental physics. Celest. Mech. Dyn. Astr. 111, 363–385. https://doi.org/10.1007/s10569-011-9377-8.

Fienga, A., Laskar, J., Exertier, P., Manche, H., Gastineau, M., 2015. Numerical estimation of the sensitivity of INPOP planetary ephemerides to general relativity parameters. Celest. Mech. Dyn. Astr. 123, 325–349. https://doi.org/10.1007/s10569-015-9639-y.

Fossat, E., Boumier, P., et al., 2017. Asymptotic g modes: Evidence for a rapid rotation of the solar core. Astron. Astrophys. 604, 17. https://doi.org/10.1051/0004-6361/201730460.

Genova, A., Mazarico, E.X., et al., 2018. Solar system expansion and strong equivalence principle as seen by the NASA MESSENGER mission. Nature Commun. 9, 289. https://doi.org/10.1038/s41467-017-02558-1.

Godier, S., Rozelot, J.P., 2001. A new outlook on the "Differential Theory" of the solar quadrupole moment and oblateness. Sol. Phys. 199, 217–229. https://doi.org/10.1023/A:1010354901960.

Hilton, J.L., Hohenkerk, C.Y., 2010. A comparison of the high accuracy planetary ephemerides DE421, EPM2008, and INPOP08. Proceedings of the Journèes 2010 Systèmes de référence spatio-temporels (JSR2010): New challenges for reference systems and numerical standards in astronomy, Observatoire de Paris, 20–22 September 2010, Edited by Nicole Capitaine, p. 77–80.

Iorio, L., 2012. Constraining the angular momentum of the sun with planetary orbital motions and general relativity. Sol. Phys. 281, 815–826. https://doi.org/10.1007/s11207-012-0086-6.

Iorio, L., 2017. Preliminary constraints on the location of the recently hypothesized new Planet of the Solar System from planetary orbital dynamics. Astrophys. Space Sci. 362 (1), 22p. https://doi.org/10.1007/s10509-016-2993-8.

Jain, K., Tripathy, S., Hill, F., 2018. The Sun's seismic radius as measured from the fundamental modes of oscillations and its implications for the TSI variations. Astrophys. J. Lett. 859, L9. https://doi.org/10.3847/2041-8213/aac327, 7 pp..

Javaraiah, J., 2003. Long-term variations in the solar differential rotation. Sol. Phys. 212, 23–49. https://doi.org/10.1023/A:1022912430585.

Kosovichev, A.K., Rozelot, J.P., 2018a. Solar cycle variations of rotation and asphericity in the near-surface shear layer. J. Atmos. Solar Terr. Phys. 176, 21–25. https://doi.org/10.1016/j.jastp.2017.08.00.

Kosovichev, A.K., Rozelot, J.P., 2018b. Cyclic Changes of the Sun's Seismic Radius. Astrophys. Jour. Lett., 861(2), 5. Article id. 90, https://doi.org/10.3847/1538-4357/aac81d, arXiv:1805.09385 [astro-ph.SR].

Kuhn, J.R., Bush, R., Emilio, M., Scholl, I.F., 2012. The precise solar shape and its variability. Science 337 (6102), 1638. https://doi.org/10.1126/science.1223231.

Lefebvre, S., Rozelot, J.P., Kosovichev, A.K., 2007. The change of solar shape in time and depth. Some consequences for space climate. J. Adv. Space Res. 40, 1000–1005. https://doi.org/10.1016/j.asr.2007.01.086.

Lustig, G., 1983. Solar rotation 1947–1981 determined from sunspot data. Astron. Astrophys. 125, 355–358.

Schettino, G., Serra, D., Tommei, A., Milani, A., 1983. Addressing some critical aspects of the BepiColombo MORE relativity experiment. Celestial Mech. Dynam. Astron., 130(11),20. https://doi.org/10.1007/s10569-018-9863-3.

Newcomb, S., 1895. In: The Elements of the Four Inner Planets and the Fundamental Constants of Astronomy (Washington, DC, USA) p. 111.

Pap, J., Kuhn, J.R., Frohlich, C., Ulrich, R. Jones, A., Rozelot, J.P., 1998. Importance of monitoring solar global properties: luminosity, radius and oscillations. In: Crossroads for European Solar and Heliospheric Physics. Recent Achievements and Future Mission Possibilities, Puerto de la Cruz, Tenerife, Canary Islands, Spain. March 23–27, 1998. European Space Agency, pp. 267–271.

Pap, J., Rozelot, J.P., Godier, S., Varadi, F., 2001. On the relation between total irradiance and radius variations. Astro. Astrophys. 372, 1005–1018. https://doi.org/10.1051/0004-6361:20010280.

Paternò, L., Sofia, S., Di Mauro, M.P., 1996. The rotation of the Sun's core. Astron. Astrophys. 314, 940–946.

Park, R.S., Folkner, W.M., Konopliv, A.S., Williams, J.G., Smith, D.E., Zuber, M.T., 2017. Precession of Mercury's Perihelion from Ranging to the MESSENGER spacecraft. Astronom. J. 153 (3), 121. https://doi.org/10.3847/1538-3881/aa5be2, 7p..

Pijpers, F.P., 1998. Helioseismic determination of the solar gravitational quadrupole moment. Monthly Notices Roy. Soc. 297, L76–L80. https://doi.org/10.1046/j.1365-8711.1998.01801.x.

Pireaux, S., Rozelot, J.P., 2003. Solar quadrupole moment and purely relativistic gravitation contributions to Mercury's perihelion advance. Astrophys. Space Sci. 284 (4), 1159–1194. https://doi.org/10.1023/A:1023673227013.

Pitjeva, E.V., 2005. Relativistic effects and solar oblateness from radar observations of planets and spacecraft. Astron. Lett. 31 (5), 340–349. https://doi.org/10.1023/A:1023673227013.

Pitjeva, E.V., 2013. Updated IAA RAS Planetary Ephemerides-EPM2011 and their use in scientific research. Solar System Research, Vol. 47, No. 5, pp. 386–402. Original Russian Text published in Astronomicheskii Vestnik, 2013, Vol. 47, No. 5, pp. 419–435.

Pitjeva, E.V., 2014. Proceedings of the "Journées des Systèmes de référence spatio-temporels": Recent developments and prospects in ground-based and space astrometry, held at Pulkovo Observatory from 22 to 24 September 2014, Z. Malkin, N. Capitaine (Eds.), pp. 92–95

Pitjeva, E.V., Pitjev, N.P., 2014b. Development of planetary ephemerides EPM and their applications. Celest. Mech. Dyn. Astr. 119 (3), 237–256. https://doi.org/10.1007/s10569-014-9569-0.

Reiter, J., Rhodes E.J. Jr., Kosovichev, A.G., Schou, J., Scherrer, P.H., Larson, T.P., 2015. A method for the estimation of p-mode parameters from averaged solar oscillation power spectra. Astrophys. J., 803–92, 42. https://doi.org/10.1088/0004-637X/803/2/92.

Rozelot, J.P., Damiani, C., Pireaux, S., 2009. Probing the solar surface: the oblateness and astrophysical consequences. Astrophys. J. 703, 1791–1796. https://doi.org/10.1088/0004-637X/703/2/1791.

Scherrer, P.H., Bogart, R.S., Bush, R.I., et al., 1995. The solar oscillations investigation-Michelson doppler imager. Solar Phys. 162, 129–188. https://doi.org/10.1007/BF00733429.

Scherrer, P.H., Schou, J., Bush, R.I., et al., 2012. The Helioseismic and magnetic imager (HMI) investigation for the Solar Dynamics Observatory (SDO). Solar Phys. 275, 207–227. https://doi.org/10.1007/s11207-011-9834.

Susuki, M., 2012. Solar rotation rate during solar activity cycle 23. Sol. Phys. 278 (2), 257–267. https://doi.org/10.1007/s11207-012-9946-3.

Standish, M., 1998. JPL Interoffice Memoradum, IOM 312.F -98-048, August 26, 1998, 18pp.

Verma, A.K., Fienga, A., Laskar, J., Manche, H., Gastineau, M., 2014. Use of MESSENGER radioscience data to improve planetary Ephemeris and to test general relativity. Astron. Astrophys. 561, A115. https://doi.org/10.1051/0004-6361/201322124.

Williams, J.G., Boggs, D.H., Folkner, W.M., 2013. JET, Interoffice Memorandum California Institute of Technology, DE430 Lunar Orbit. Physical Librations, and Surface Coordinates, IOM 335-JW, DB, WF-20080314-001.

Xu, Y., Shen, Y., Xu, G., Shan, X., Rozelot, J.P., 2017. Monthly Notices Roy. Soc. 472, 2686–2693. https://doi.org/10.1093/mnras/stx2122.